Nonlinear Conversion Efficiency of InAs/InP Nanostructured Fabry-Perot Lasers

Heming Huang[a*], Kevin Schires[a], Mohamed Chaibi[a], Philip Poole[b], Didier Erasme[a], and Frédéric Grillot[a]

[a]Telecom Paristech, Ecole Nationale Supérieure des Télécommunications, CNRS LTCI, 46 rue Barrault, 75013 Paris, France
[b]NRC Canada, 1200 Montreal Road, Building M-50, Room 162, Ottawa, Canada

heming.huang@telecom-paristech.fr

ABSTRACT

Non-degenerate four-wave mixing effects are investigated in an injection-locked InAs/InP nanostructure Fabry-Perot laser. Locking a longitudinal mode at various wavelengths within the gain spectrum and using the locked mode as the pump for the wave mixing shows different levels of asymmetry between up- and down-conversion. Experiments reveal that the normalized conversion efficiency is less asymmetric when the pump is locked at wavelengths below that of the gain peak. The values of nonlinear conversion efficiencies are maintained above -60 dB for pump-probe frequency detunings up to 3.5 THz. The role of the linewidth enhancement factor on the asymmetry is discussed and the value of the nonlinear susceptibility is compared to similar InAs/InP nanostructure semiconductor optical amplifiers. From an end-user viewpoint, data transmission experiments have also confirmed the possibility to propagate up-converted signals over 100 km at a 5 Gb/s bit rate under an OOK modulation format.

Keywords: semiconductor lasers, quantum dots, four-wave mixing, injection-locking, transmission

1. INTRODUCTION

Non-degenerate four-wave mixing (NDFWM) is a nonlinear interaction process driven by the third-order nonlinear susceptibility $\chi^{(3)}$. In semiconductor media, four-wave mixing has been extensively used to produce wavelength conversion for wavelength division multiplexed (WDM) systems, to balance chirping characteristics in semiconductor optical amplifiers (SOA) and to generate self-pulsation with high repetition rates through passive mode locking [1]-[3]. Due to the beating between the pump and probe signals, NDFWM leads to additional waves that behave as the converted conjugate replica of the input signals. When the frequency detuning (Δf) between the pump and probe lies within a few GHz [4], NDFWM is mostly governed by the carrier density pulsation (CDP) from which the beating between the pump and probe waves creates temporal gain and index gratings. For larger frequency detunings up to the THz range [5], spectral hole burning (SHB) and carrier heating (CH) become the dominant mechanisms within sub-picosecond timescales. The former is connected to the gain saturation effects and intra-band scattering while the latter produces a beating of the carrier temperature via phonon scattering. Although values of $\chi^{(3)}$ are always higher for low frequency detunings due to the larger contribution of the CDP, the very large bandwidth offered by the CH and SHB is also promising for broadband wavelength conversion. In contrast to quantum well (QW) materials, quantum dots (QDs) do exhibit various advantages such as a wider gain spectrum [6], ultrafast carrier dynamics [5], higher nonlinear gain effect and a larger third-order nonlinear susceptibility [7]-[9]. In addition, due to the reduced linewidth enhancement factor (LEF) or α_H-factor, QD nanostructures are useful for eliminating destructive interferences among the different nonlinear processes, hence lowering the asymmetry between up- and down-converted signals [10]. Most experimental studies of four-wave mixing have been performed in SOAs with bulk, QW and QD structures. Generally, while SOAs have a larger linear gain providing higher conversion efficiency, the wavelength conversion remains limited by their strong amplified spontaneous emission (ASE) noise. In such way, there is always an optimum linear gain that can maximize the conversion efficiency to noise ratio, while a tradeoff on the pump power is also required to obtain a better performance. On the other hand, a laser cavity exhibits a reduced ASE through resonance and can thus provide a higher optical signal-to-noise ratio (OSNR) with respect to SOAs. To this end, this paper aims at extending the study of NDFWM [11] to semiconductor laser diodes in order to show that further improvements in the NDFWM generation as well as to a higher

optical signal-to-noise ratio (OSNR) can be achieved. Although the use of a DFB laser is simpler, given that its single lasing peak can be employed as pump wave, it has to be stressed that in this case the nonlinear efficiency remains strongly dependent on some complex additional DFB features such as the strength of the grating coefficient, facet phase effects or spatial hole burning, which are somewhat difficult to control from device to device [7][12][13]. FP lasers are thus good candidates for NDFWM, providing that the pump wave generated by optical injection-locking (OIL) is a single longitudinal mode. This allows in fact at the same time an improvement of the properties of the locked laser by reducing its spectral linewidth or frequency chirp, as well as the relative intensity noise and the nonlinear distortion [14][15][16]. In this work, a dual-injection technique is employed in a 1550 nm InAs/InP QD Fabry-Perot (FP) laser operating within the stable-locking range. The NCE is found to vary from -25 dB to -60 dB for frequency detunings ranging from a few tens of GHz to several THz. The locked QD FP laser thus allows efficient wavelength conversion for frequency detunings much larger than those achieved with QD SOAs [9]. Locking the pump signal at different wavelengths within the gain curve shows different asymmetry between up- and down-conversion. When a longitudinal mode locked at wavelengths shorter than the gain peak is used as pump the asymmetry is weaker, as opposed to the situation arising at longer wavelengths. From the measured normalized conversion efficiency (NCE) and SNR, the role of linewidth enhancement factor is discussed. Moreover, the converted signal is used in a modulation platform for transmission experiments where 5Gb/s open eye diagrams are reported after propagation over a 100 km optical fiber.

2. STATIC LASER CHARACTERIZATIONS

The device under study is an InAs/InP QD FP laser. The active region is made of five InAs QD layers grown by chemical beam epitaxy (CBE) on a (100)-oriented n-type InP substrate. The ridge optical waveguide is L=1 mm long and 3 μm width with cleaved facets (R=0.32). Figure 1(a) represents the coupled output power per facet of the laser measured at 293K. The threshold current is I_{th}=39 mA and the external quantum efficiency per facet is about 16%. Figure 1(b) gives the corresponding optical spectrum of the free-running laser showing a peak emission centered at 1543 nm.
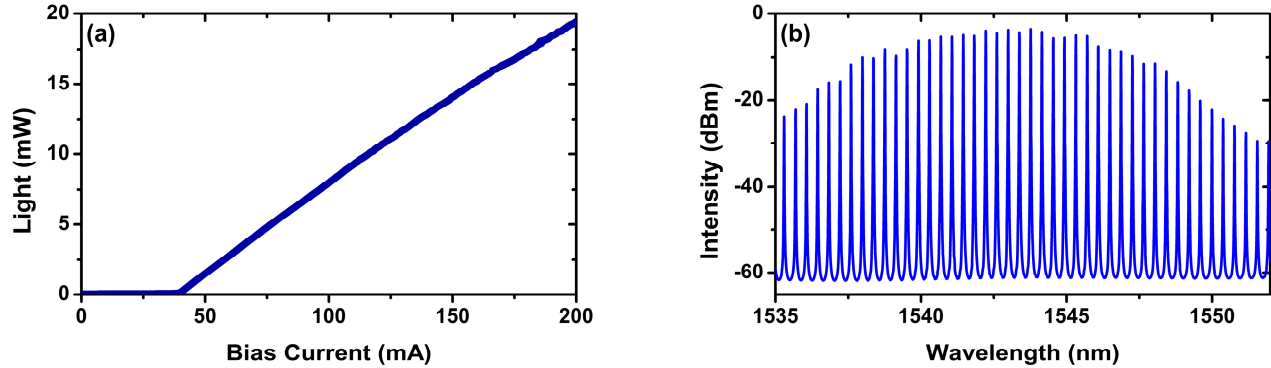

Figure 1. (a) The light current characteristic; (b) The optical spectrum recorded of the InAs/InP QD laser at 293K

Below threshold, the optical gain of the laser increases with the pump current I, while it is clamped above threshold. By measuring the evolution of both the wavelength λ and the gain for various bias currents, the below threshold α_H-factor of the laser can be determined by:

$$\alpha_H = -\frac{2\pi}{L\Delta\lambda}\frac{d\lambda/dI}{dg_{net}/dI} \qquad (1)$$

where g_{net} is the net modal gain, which can be obtained from the Hakki-Paoli method. This method is based on the peak-to-valley ratio of the amplified spontaneous spectrum (ASE), and the net modal gain g_{net} is extracted using the following relationship:

$$g_{net} = \Gamma_p g - \alpha_i = \frac{1}{L} \ln\left(\frac{1}{R} \frac{\sqrt{x} - 1}{\sqrt{x} + 1} \right) \tag{2}$$

where g is the material gain, α_i the internal loss coefficient, and Γ_p is the optical confinement factor and x the ratio of the peak-to-valley intensity levels. Figure 2 shows the net modal gain variation of the QD laser under test from I_{bias}=25 mA to I_{bias}=39 mA with a current step of 2 mA. At threshold, the net modal gain is of 11 cm^{-1} at the gain peak. The figure in inset represents the evolution of the below-threshold LEF as a function of the lasing photon wavelength. After elimination of the thermal effects, the LEF is found to increase from 0.7 to 2.2 with a relatively low value of 1.4 at the gain peak.
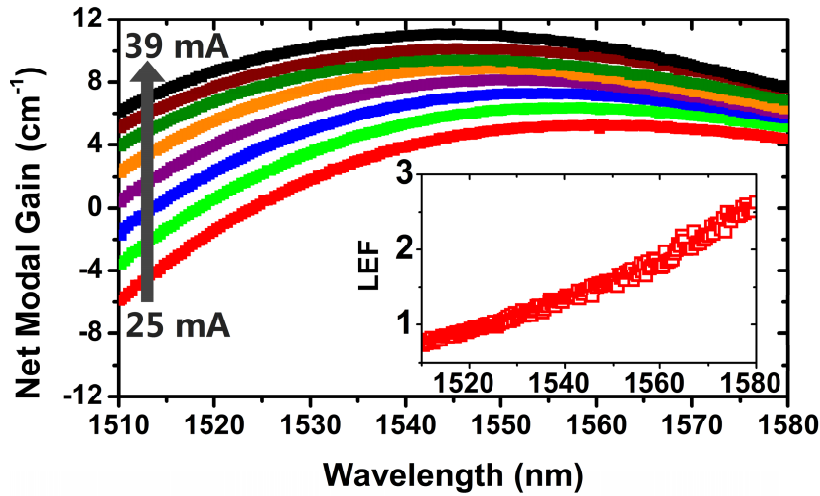
Figure 2. Measured net modal gain for different pump currents; The figure in inset shows the below-threshold linewidth enhancement factor (LEF) of the QD laser under study

3. FOUR-WAVE MIXING CONVERSION EFFICIENCY

Figure 3 shows a schematic of the experimental setup. The light from two tuneable lasers, TL1 and TL2, is merged through an 80/20 coupler, and injected into the slave QD FP through an optical circulator and a lens-ended fibre, used to both inject the light into the QD FP and collect the light it emits. TL1 is used as master laser in order lock a single longitudinal mode of the FP around its gain peak and use it as pump for the wave mixing. TL2 is then used as probe to generate the four-wave mixing with the locked FP mode. The polarisations of both tuneable lasers were set to match that of the slave laser using fibre polarisation controllers. The NDFWM spectra are then measured using an optical spectrum analyzer (OSA) with a 10 pm resolution at port 3 of the circulator.
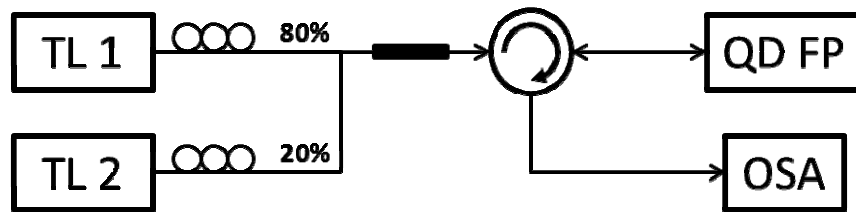
Figure 3. Experimental setup used for the non-degenerate four-wave mixing (NDFWM)

In this paragraph, the QD FP laser is biased at 2.5×I_{th} at 293K The injected power from TL1 is set 3 dB below that of the free-running slave QD FP, and its wavelength is set 80 pm above that of the targeted mode. The injected power from

TL2 was set at 450 µW. The difference in frequency between the locked mode of the FP and TL2, equal to the detuning between TL1 and TL2, defines the NDFWM detuning Δf. Figure 4 presents the two types of wavelength conversion. In Figure 4 (a), the probe wave is at a lower wavelength than the locked pump mode and Δf is thus negative. The converted signal having a lower frequency than the probe, the situation is referred to as down-conversion. Figure 4 (b) presents the opposite situation, where Δf is positive and the converted signal has a frequency that is higher than that of the pump, which is referred to as up-conversion.
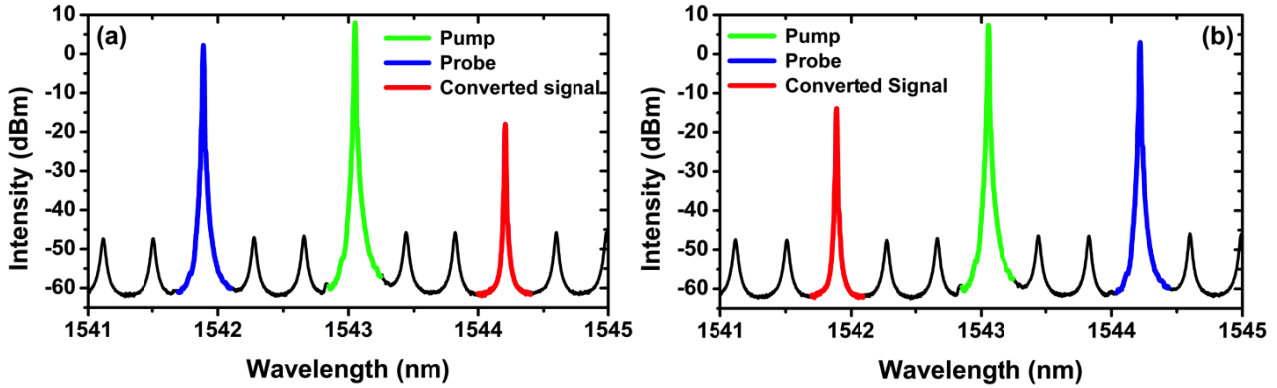

Figure 4. NDFWM optical spectra measured for ±150 GHz frequency detunings with the pump locked at 1543 nm: (a) -150 GHz detuning, down-conversion; (b) +150 GHz detuning, up-conversion

The normalized conversion efficiency (NCE) is expressed, in mW^{-2}, as [16]:

$$\eta_{NCE} = \frac{P_{converted\ signal}}{P_{pump}^2 P_{probe}}$$

(3)

In Eq. (1), optical powers are defined after propagation within the active region, and are traditionally measured using the peak powers in the experimental optical spectra. As the NCE is not a mere ratio of powers but is normalized to the squared power of the pump, the optical losses between the facet of the FP and the input of the OSA need to be measured in order to estimate the actual power of the pump wave. Failing to do so would lead to an overestimation of the NCE.

Figure 5 (a) presents the evolution of the NCE for a range of values of Δf when the mode at the gain peak is used as pump wave. The frequency detuning is here given in absolute value, the NCE for up- (resp. down-) conversion being shown in red (blue). The conversion is more efficient when the CDP mechanism dominates, for detunings of a few GHz, with a maximum NCE of about -25 dB. Most importantly, a NCE above -45 dB (horizontal dot line in Figure 5 (a)) is achieved between -500 GHz and +1.5 THz. At larger frequency detunings, SHB and CH dominate and allowing a weaker conversion with NCEs above -60 dB for detunings between -2.5 THz and +3.5 THz. Figure 5 (b) shows the OSNR, defined as the power ratio between the converted signal and the surrounding side-modes. While OSNRs above 20 dB are achieved between -500 GHz and +1.5 THz (up-conversion), the converted signal quickly sinks down to the noise level for absolute detunings above 2 THz. Compared to similar InAs/InP nanostructured SOAs, the experiments show a larger OSNR associated to a clear extension of the NDFWM frequency detuning range further in the THz window, without the need of using of very long interaction lengths [9].
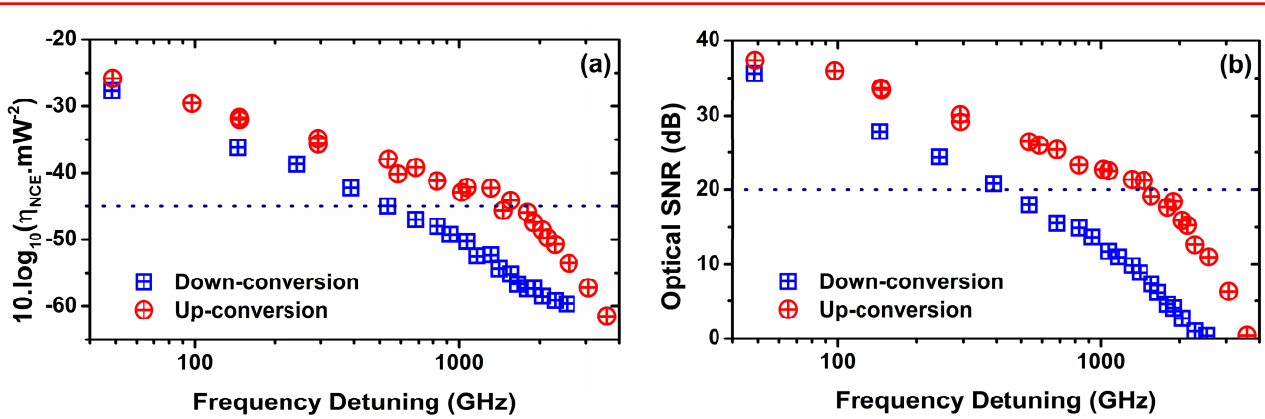
Figure 5. The measured NCE (a) and OSNR (b) as a function of the pump-probe frequency detuning

Figure 5(a) also shows a reduced asymmetry between up- and down-conversion profiles as compared to bulk or QW SOAs, which reach a maximum difference of 15 dB around 1.5 THz of detuning. This phenomenon can be attributed to the reduced LEF measured on this InAs/InP QD laser [16], [17] from which a lower phase between nonlinear processes can lead to constructive interferences and to a nonlinear conversion less dependent on the sign of the detuning as shown. To this end, Figure 5(a) shows that the down converted signals decay a bit faster than the up-converted one since the former experiences a larger LEF as reported in the inset of the figure 2.

As the LEF varies over the whole gain spectrum, the impact of the pump wavelength on the conversion efficiency has been investigated in order to study the effect of the LEF on this asymmetry. In addition to using the mode at the gain peak as pump wave, we repeated the NDFWM measurements using modes 5 nm on each side of the gain peak as pump waves, namely 1538 and 1548 nm. These modes were locked by TL1 using the same injection conditions, and similar ranges of detunings between TL1 and TL2 were studied.

Figure 6 shows the NCE profiles of (a) up- and (b) down-conversion for the three pump wavelengths studied. Compared to the results obtained with a pump at the gain peak, the NCE obtained for a pump at 1548 nm is higher in the case of up-conversion and lower in the case of down-conversion. While this shows that a more efficient up-conversion is achievable for detunings further into the THz window when using a pump at a wavelength above the gain peak, it also implies that the asymmetry between up- and down-conversion has increased. On the other hand, while the up-conversion is less efficient when using a pump at 1538 nm than at the gain peak, down-conversion becomes more efficient and the asymmetry is thus reduced. This result agrees well with the measurement of the LEF spectrum presented in Figure 2(b): a lower LEF is measured below the gain peak wavelength hence a reduced asymmetry between up- and down-conversion is expected when using a pump at a shorter wavelength.
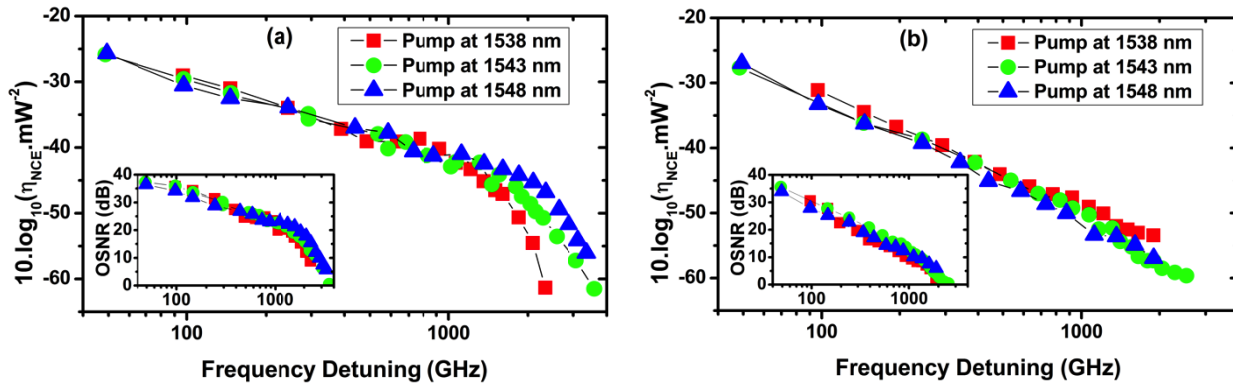
Figure 6. (a) NCE for up-conversion measured for different pump wavelength; (b) NCE of the down-conversion measured for different pump wavelength. The insets represent the corresponding OSNRs

4. TRANSMISSION EXPERIMENTS

This section investigates the dynamical characteristics of an up-converted signal were tested under 2.5 Gb/s and 5 Gb/s On-Off-Keying (OOK) modulation formats. The conversion was performed with a rather short Δf of 100 and 200 GHz in order to obtain an NCE close to -30 dB. In such a frequency range, the wavelength of the pump wave has little impact on the NCE and the mode at the gain peak was used as pump.

Figure 7 represents the experimental setup, which is an extended version of that presented in Figure 3 where the light of TL2 is modulated using an external Mach-Zehnder Modulator (MZM). A pulse pattern generator (PPG) was used to modulate the light from TL2 and trigger a high-resolution sampling scope. Before the oscilloscope, an optical band pass filter with a 240 pm width was used to filter out the pump and probe waves as well as the ASE of the EDFAs. The eye diagram of the modulated converted signal was then measured under the two bit rates studied and for propagation in SMF fibers of two different lengths (one of a few meters and another one of 100 km).
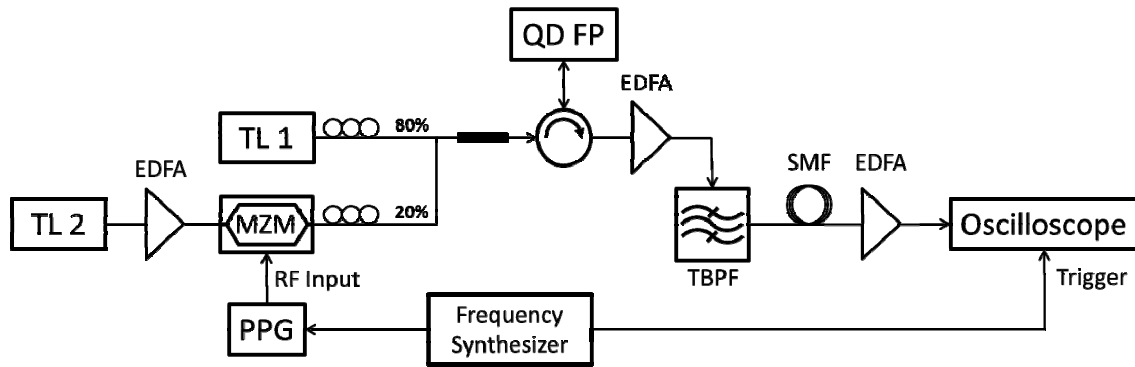
Figure 7. Experimental setup used for the transmission experiments

Table 1 shows different eye diagrams recorded under various conditions. With a 2.5 Gb/s bit rate, the eye diagram remains widely open even after 100 km transmission with a clear separation of the 1 and 0 levels. However, due to the relaxation oscillation in the QD gain medium, over-shoot peaks are observed for both detuning conditions. At 5 Gb/s, the eye diagram at 100 GHz is less opened than at 200 GHz. This phenomenon is that at 200 GHz, the sub-picosecond SHB and CH mechanisms begin to dominate, while at 100 GHz the CDP remains the leading mechanism [5]. However, although the nonlinear conversion is better at 100 GHz, the degradation of the eye diagram at 100 GHz may also be due to optical noise during the reception. As a consequence, results depicted in the table 1 do prove that the 200 GHz detuned signal can even support faster modulation than 100 GHz. To this end, in order to verify the stability of the transmission platform, the eye diagrams were taken on different days and found reproducible. These results indicate the possibility of using QD laser as wavelength converter in WDM systems.

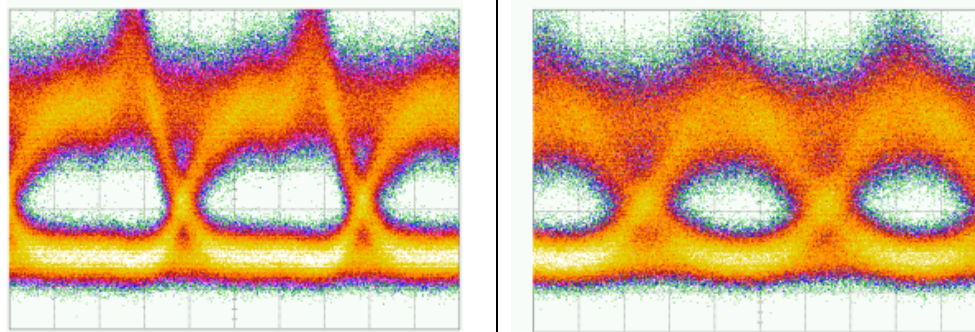| Detuning	2.5 Gb/s over 100 km fiber	5 Gb/s over 100 km fiber
100 GHz		
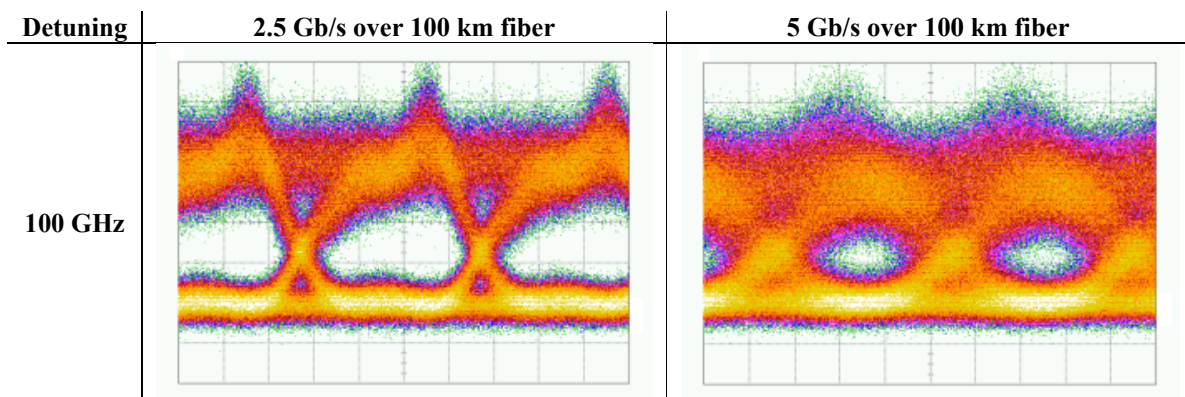
200 GHz

Table 1. Eye diagrams with a Δf of 100 and 200 GHz and under 2.5 Gb/s and 5 Gb/s over 100 km across a standard SMF optical fiber.

5. CONCLUSIONS

In this paper, a comprehensive NDFWM study is reported in an InAs/InP QD FP laser employing an optical injection-locking scheme. Taking advantage of the SHB and CH mechanisms driven by fast carrier-carrier and carrier-phonon scatterings[5], we show that a laser cavity allows extending the detuning range up to 3.5 THz as well as maintaining an NCE above -40 dB up to 1.5 THz with a large OSNR above 20 dB. The measured NCEs are found to be higher than the ones obtained with QD SOAs grown on the same material system[6]. In addition, selecting longitudinal modes of the FP at various positions in the gain spectrum allows either reducing the asymmetry between up- and down-converted signals or increasing the up-conversion efficiency. From an end-user viewpoint, experiments have confirmed the possibility to propagate 5 Gb/s OOK up-converted signals over 100 km with a wide eye diagram. Further work will concentrate on the analysis of the transmission capabilities of the converted signals at other pump wavelength and larger detunings, as well as on the nonlinear conversion efficiency provided by the first excited level of the quantum nanostructures.

ACKNOWLEDGMENTS

REFERENCES

[1] D. D. Marcenac, D. Nesset, A.E. Kelly, M. Brierley, A.D. Ellis, D.G. Moodie, and C.W. Ford, "40 Gbit/s transmission over 406 km of NDSF using mid-span spectral inversion by four-wave mixing in a 2mm long semiconductor optical amplifier", Electron. Lett., **33**, 879-880, (1997)
[2] H. Soto and D. Erasme, "Investigation of nondegenerate four wave mixing in semiconductor optical amplifier through bias current modulation", Appl. Phys. Lett., 68, 3698 (1996)
[3] J. Renaudier, G.H. Duan, J.G. Provost, H. Debregeas-Sillard, and P. Gallion, "Phase correlation between longitudinal modes in semiconductor self-pulsating DBR lasers", IEEE Photon. Technol. Lett., **17**, 741-743 (2005)
[4] G.P. Agrawal, "Population pulsations and nondegenerate four-wave mixing in semiconductor lasers and amplifiers", JOSA B, **5**, 147-159 (1988)
[5] D. Nielsen and S.L. Chuang, "Four-wave mixing and wavelength conversion in quantum dots", Phys. Rev. B, **81**, 035305 (2010)
[6] H. Li, G. T. Liu, P. M. Varangis, T. C. Newell, A. Stintz, B. Fuchs, K. J. Malloy, and L. F. Lester, "150-nm tuning range in a grating-coupled external cavity quantum-dot laser", IEEE Photon. Technol. Lett., 12, 759–761 (2000)
[7] H. Su, H. Li, L. Zhang, Z. Zou, A. L. Gray, R. Wang, P. M. Varangis, and L. F. Lester, "Nondegenerate Four-Wave Mixing in Quantum Dot Distributed Feedback Lasers", IEEE Photon. Technol. Lett., **17**, 1686–1688 (2005)
[8] T. Akiyama, O. Wada, H. Kuwatsuka, T. Simoyama, Y. Nakata, K. Mukai, M. Sugawara, and H. Ishikawa, "Nonlinear processes responsible for nondegenerate four-wave mixing in quantum-dot optical amplifiers", Appl. Phys. Lett., **77**, 1753–1755 (2000)

[9] Z. G. Lu, J. R. Liu, S. Raymond, P. J. Poole, P. J. Barrios, D. Poitras, F. G. Sun, G. Pakulski, P. J. Bock, and T. Hall, "Highly efficient non-degenerate four-wave mixing process in InAs/InGaAsP quantum dots", Electron. Lett., **42**, 1112–1113 (2006)

[10] C. H. Lee, Microwave Photonics, CRC Press (2007)

[11] C. Wang, F. Grillot, F. Y. Lin, I. Aldaya, T. Batte, C. Gosset, E. Decerle, and J. Even, "Nondegenerate Four-Wave Mixing in a Dual-Mode Injection-Locked InAs/InP(100) Nanostructure Laser", IEEE Photon. J., **6**, 1500408 (2014)

[12] A. Mecozzi, A. D'Ottavi, and R.Q. Hui, "Nearly Degenerate Four-Wave Mixing in Distributed Feedback Semiconductor Lasers Operating Above Threshold", IEEE J. Quantum Electron., **29**, 1477–1487 (1993)

[13] T. Simoyama, H. Kuwatsuka, and H. Ishikawa, "Cavity Length Dependence of Wavelength Conversion Efficiency of Four-Wave Mixing in λ/4-shifted DFB Laser", FUJISU Sci. Tech. J., **34**, 235–244 (1998)

[14] G. Yabre, "Effect of relatively strong light injection on the chirp-to-power ratio and the 3 dB bandwidth of directly modulated semiconductor lasers", J. Lightw. Tech., **14**, 2367–2373 (1996)

[15] T. B. Simpson, J. M. Liu, and A. Gavrielides, "Bandwidth Enhancement and Broadband Noise Reduction in Injection-Locked Semiconductor Lasers", IEEE Photon. Technol. Lett., **7**, 709–711 (1995)

[16] X. J. Meng, T. Chau, and M. C. Wu, "Improved Intrinsic Dynamic Distortions in Directly Modulated Semiconductor Lasers by Optical Injection Locking", IEEE Trans. Microw. Theory Tech., **47**, 1172–1176 (1999)

[17] T. Akiyama, H. Kuwatsuka, N. Hatori, Y. Nakata, H. Ebe, and M. Sugawara, "Symmetric Highly Efficient (~0 dB) Wavelength Conversion Based on Four-Wave Mixing in Quantum Dot Optical Amplifiers", IEEE Photon. Technol. Lett., **14**, 1139–1141 (2002)